Supporting Information

Fabrication of Polyaniline Nanofiber Array on Poly(etheretherketone) to Induce Enhanced Biocompatibility and Controlled Behaviours of Mesenchymal Stem Cells

Hainan Gao,[a] Junhu Zhang,[*a] Fangyuan Liu,[a] Zhuo Ao,[b] Sidi Liu,[a] Shoujun Zhu,[a] Dong Han,[*b] and Bai Yang [a]

Figure S1. a) Static-water contact angle (n=5) of PAAc-PEEK and ANI-PAAc-PEEK after immersion in ANI monomer *vs.* the photo-irradiation time in AAc monomer.

Figure S2. By controlling the photo-irradiation time in AAc monomers, different amount of COOH- group can be obtained on PEEK surface, which can have great impact on PANI nanotopographies. The schematic below illustrates the polymerization modes of PANI on PEEK with different amount of -COOH. By controlling photo-irradiation time at 1.5 min, the amount of PAAc on PEEK was appropriate to anchoring PANI tough and still maintaining the long-range order of PANI nanofiber arrays.

Figure S3. SEM images of various PANI nanofibers on PAAc-PEEK. The photo-irradiation time in AAc monomers was 0, 1.5, and 6 min; A and C group has the PANI monomer concentration at 4 and 20 mM respectively during the polymerization of PANI.

Figure S4. Typical force versus distance curves to evaluate BSA protein-substrate adhesion work extracted from different surfaces.

Figure S5. Tilted view for the interface of rMSCs and PANI-A. The effective contacts of cell/nanofibers were shown mostly on the top of nanofibers. Contact guidance is a leading example of a naturally occurring phenomenon that is characterized by the response of cells to structures on the micrometer and sub-micrometer scale. Contact guidance is an essential component in regulating cell migration, which is modulated by organized ECM proteins. The SEM image below displays the contact joint of cell and nanofibers. There are a lot of micro-protrusions forming from the bottom of cell to generate effective contact with nanofibers, and the effective contact is matched nanofiber dimensions, which can further confirmed the normalized effective-area (EA) model.

Experimental Section

Cell morphological characterization by SEM. The cells growing on the substrates were washed with 1×PBS and fixed with 2.5% (v/v) glutaraldehyde for 30 min. After fixation, they were washed 3 times with 1×PBS for 5 min each wash. Then the cells were dehydrated in a graded series of ethanol (50, 70, 85, 90, and 100 v%) for 20 min each and left in 100% ethanol until they were dried by CO_2 critical point dryer (BAL-TEC CPD030). The morphologies of the adhering cells were observed by an environmental scanning electronic microscope (ESEM) under low-vacuum MODE (Quanta 200 FEG, FEI Co.).

Immunofluorescence of Actin/vinculin/DAPI. The rMSCs on the bare PEEK and PANI nanofiber substrates were fixed in 4% (w/v) paraformaldehyde in 1×PBS for 20 min at room temperature. Once fixed, the cells were washed twice with 1×PBS containing 0.05% (v/v) Tween-20. To permeablilize the cells 0.3% (v/v) Triton X-100 in 1×PBS solution was added for 10 min at 0-4°C. The cells were washed twice with 1×PBS wash buffer. Then the samples were incubated for 2 h at room temperature in 3% (w/v) BSA/1×PBS followed by the addition of vinculin antibody (1: 100, Sigma), and incubated for overnight at 4 °C. After incubation, cells were washed 3 times for 5 min each wash with 1×PBS wash buffer. Goat antimouse IgG-FITC (1:100, Santa Cruz Biotechnology) and TRITC-conjugated phalloidin (1:40, Invitrogen) in 1×PBS was added for double staining and the cells were incubated again for 1h at room temperature. The cells were washed 3 times with 1×PBS wash buffer for 5 min each wash. Then, the samples were stained by DAPI (1:1000, Chemicon) for 3-5 min for nucleus staining. At last the samples were mounted on microscope slides and analyzed by fluorescence microscopy (Nikon) equipped with DG-4 (Sutter Instrument) and 40×oil immersion lens, using the software MetaMorph 7.0.

Figure S1. a) Static-water contact angle (n= 5) of PAAc-PEEK and ANI-PAAc-PEEK after immersion in ANI monomer *vs.* the photo-irradiation time in AAc monomer.

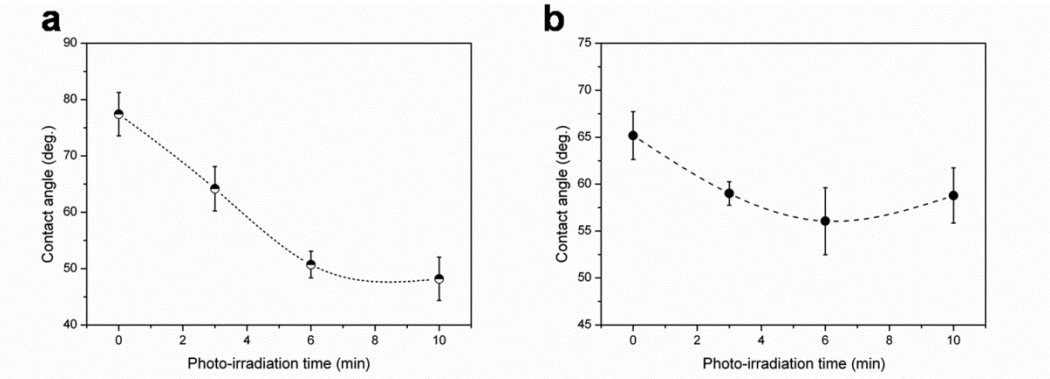

The water-wettability of the PAAc-PEEK surface is considerably greater than that of the untreated PEEK surface (Figure S1 a), because PAAc is a highly hydrophilic compound with COOH group. The corresponding water-wettability of ANI-PAAc-PEEK was dependent on the photo-irradiation of PEEK in AAc. We observed that the adhesion intensity between PANI and PEEK was greatly dependent on the water-wettability (the amount of COO^- on PEEK). However, the nanotopographies of PANI growing on PEEK with various amount of COO^- were distinct.

Figure S2. By controlling the photo-irradiation time in AAc monomers, different amount of COOH group can be obtained on PEEK surface, which can have great impact on PANI nanotopographies. The schematic below illustrates the polymerization modes of PANI on PEEK with different amount of COOH-. By controlling photo-irradiation time at 1.5 min, the amount of PAAc on PEEK was appropriate to anchoring PANI tough and meanwhile maintaining the long-range order of PANI nanofibers.

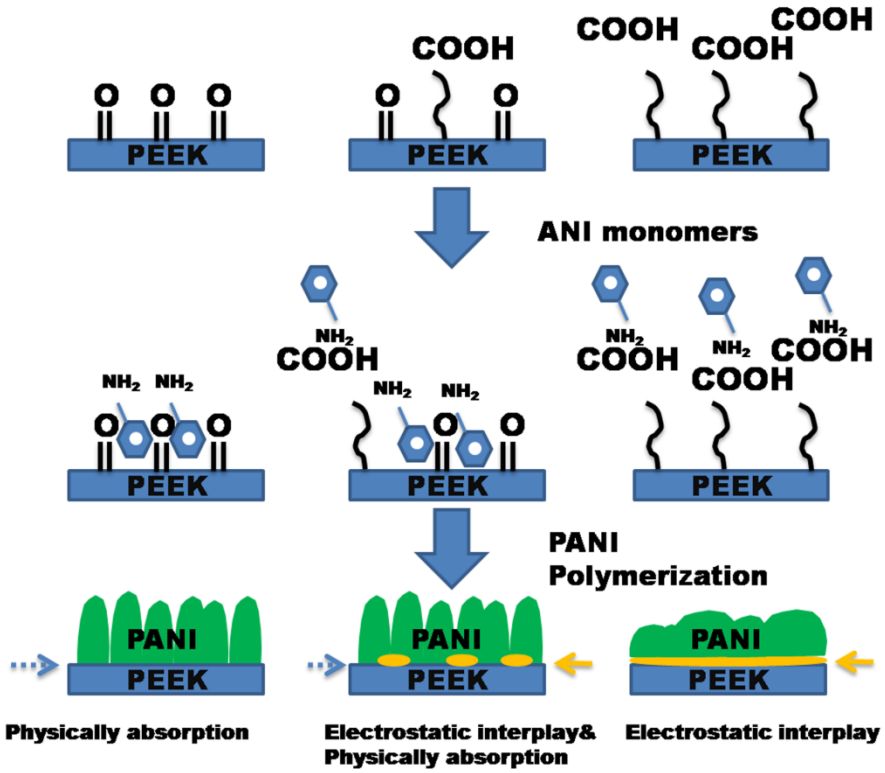

Figure S3. SEM images of various PANI nanofibers on PAAc-PEEK. The photo-irradiation time in AAc monomers was 0, 1.5, and 6 min; A and C group has the PANI monomer concentration at 4 and 20 mM respectively during the polymerization of PANI.

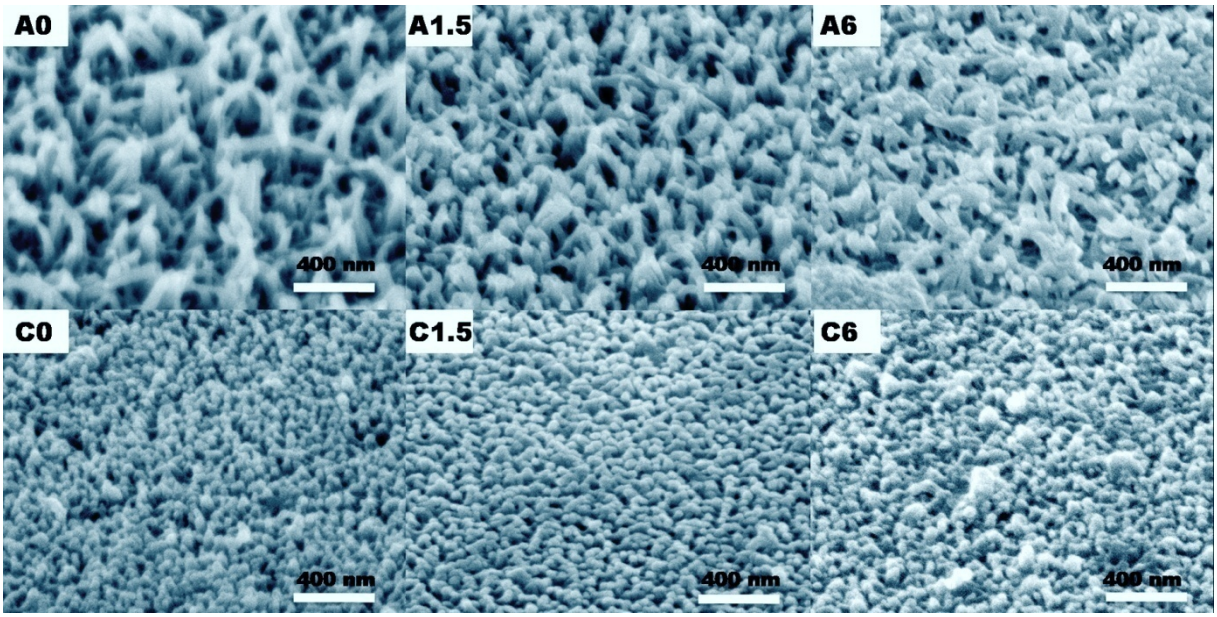

Figure S4. Typical force versus distance curves to evaluate the adhesion work of BSA protein-substrates extracted from different surfaces.

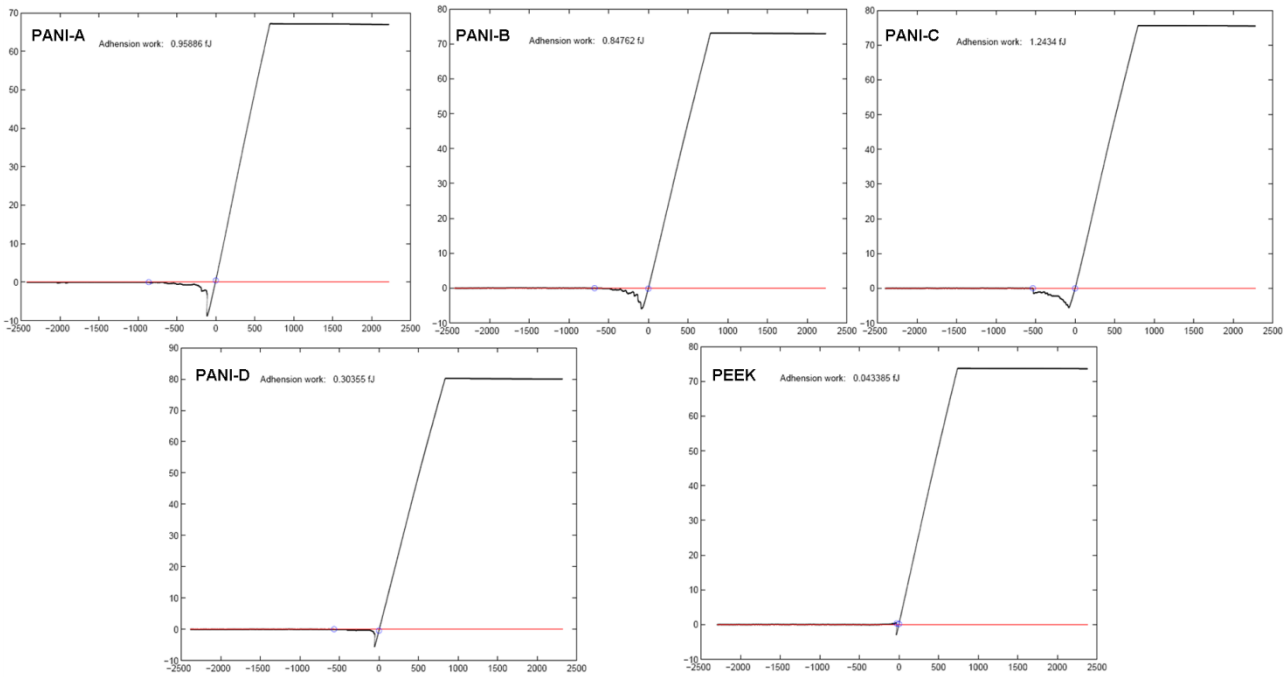

Figure S5. Contact guidance is a leading example of a naturally occurring phenomenon that is characterized by the response of cells to structures on the micrometer and sub-micrometer scale. Contact guidance is an essential component in regulating cell migration, which is modulated by organized ECM proteins. The SEM image below displays the sophisticated contact of cell/nanofibers. There are a lot of micro-protrusions forming from the bottom of cell to generate effective contact with nanofibers, and the effective contact is matched nanofiber dimensions, which can further confirmed the normalized effective-area (EA) model.